

Received 27 August; accepted 23 December 1992.

1. Prentice, K. C. & Fung, Y. I. *Nature* **346**, 48–51 (1990).
2. Smith T. M., Leemans, R. & Shugart, H. H. *Clim. Change* **21**, 367–384 (1992).
3. Hansen, J. et al. *J. geophys. Res.* **93**, 9341–9364 (1988).
4. Manabe, S. & Wetherald, R. T. *J. atmos. Sci.* **44**, 1211–1235 (1987).
5. Olson, J. S., Watts, J. A. & Allison, L. J. *Carbon in Live Vegetation of Major World Ecosystems*, Rep. ORNL-5862 (Oak Ridge National Laboratory, Oak Ridge, TN, 1983).
6. Schlesinger, W. H. in *The Changing Carbon Cycle: A Global Analysis* (eds Trabalka, J. R. & Reichle, D. E.) 194–220 (Springer, New York, 1986).
7. Emanuel, W. R., Shugart, H. H. & Stevenson, M. P. *Clim. Change* **7**, 29–43 (1985).
8. Holdridge, L. R. *Life Zone Ecology* (Tropical Science Center, San Jose, Costa Rica, 1967).
9. Leemans, R. & Cramer, W. *The IIASA Climate Database for Land Area on a Grid of 0.5° Resolution*, WP-41 (International Institute for Applied Systems Analysis, Laxenburg, Austria, 1990).
10. Post, W. M., Emanuel, W. R., Zinke, P. J. & Stangenberger, A. G. *Nature* **346**, 48–51 (1983).
11. Peng, T. H., Broecker, W. S., Freyer, H. D. & Trumbore, S. *J. geophys. Res.* **88**, 3609–3620 (1983).
12. Goudriaan, J. & Ketner, P. *Clim. Change* **6**, 167–192 (1984).
13. Emanuel, W. R., Killough, G. G., Post, W. M. & Shugart, H. H. *Ecology* **65**, 970–983 (1984).
14. Houghton, R. A., et al. *Ecol. Monogr.* **53**, 235–262 (1983).
15. Shugart, H. H. *A Theory of Forest Dynamics* (Springer, New York, 1984).
16. Shugart, H. H., Emanuel, W. R., West, D. C. & DeAngelis, D. L. *Math. Biosci.* **50**, 163–170 (1980).
17. Solomon, A. M. *Oecologia* **68**, 567–569 (1986).
18. Bonan, G. B. & Hayden, B. P. *Quat. Res.* **33**, 204–218 (1990).
19. Smith, T. M., Bonan, G. B., Shugart, H. H. & Smith, J. B. *Adv. ecol. Res.* **22**, 93–116 (1992).
20. Davis, M. B. in *Forest Succession* (eds West, D. C., Shugart, H. H. & Botkin, D. B.) 132–151 (Springer, New York, 1981).
21. Davis, M. B. *Clim. Change* **15**, 75–82 (1989).

Active volcanism beneath the West Antarctic ice sheet and implications for ice-sheet stability

Donald D. Blankenship*, Robin E. Bell†,
Steven M. Hodge‡, John M. Brozena§,
John C. Behrendt|| & Carol A. Finn||

* Institute for Geophysics, The University of Texas at Austin, Austin, Texas 78759, USA

† Lamont-Doherty Earth Observatory of Columbia University, Palisades, New York 10964, USA

‡ U.S. Geological Survey, Tacoma, Washington 98406, USA

§ Naval Research Laboratory, Washington DC 20375, USA

|| U.S. Geological Survey, Denver, Colorado 80225, USA

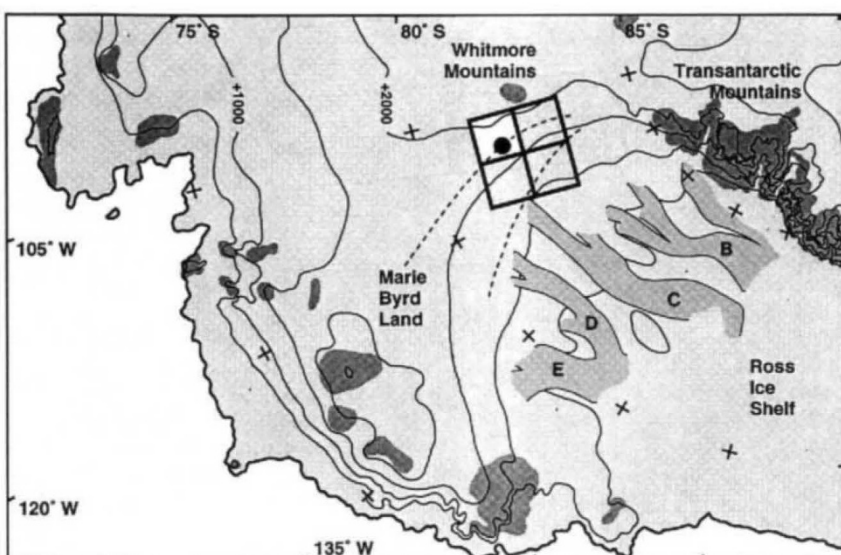
IT IS widely understood that the collapse of the West Antarctic ice sheet (WAIS) would cause a global sea level rise of 6 m, yet there continues to be considerable debate about the detailed response of this ice sheet to climate change^{1–3}. Because its bed is grounded well below sea level, the stability of the WAIS may depend on geologically controlled conditions at the base which are independent of climate. In particular, heat supplied to the base of the ice sheet could increase basal melting and thereby trigger ice streaming, by providing the water for a lubricating basal layer of till on which ice streams are thought to slide^{4,5}. Ice streams act to protect the reservoir of slowly moving inland ice from exposure to oceanic degradation, thus enhancing ice-sheet stability. Here we present aerogeophysical evidence for active volcanism and

FIG. 1 Map of a portion of the West Antarctic ice sheet¹⁷ with the ice sheet and ice shelves lightly shaded. The South Pole is marked by a box in the upper right corner and the surface elevations are shown with 500-m contours. The approximate regions of exposed bedrock are darkly shaded while the intermediate shading indicates the ice streams of the interior Ross embayment between Marie Byrd Land and the Transantarctic Mountains. The ice streams are identified as B through E from south to north and the western Byrd subglacial basin is located between Marie Byrd Land and the Whitmore Mountains. The West Antarctic rift system is considered to be the region bounded by Marie Byrd Land to the north and by the Transantarctic Mountains to the south and west. In the southeast, it is thought to be bounded by the elevated Ellsworth–Whitmore crustal block which includes the Whitmore Mountains. The CASERTZ aerogeophysical surveying of 1991–92 was accomplished within the four highlighted blocks; the survey block indicated by the white square contains the north–south profile of Fig. 2 and encompasses the area shown in Fig. 4. For each one-degree survey block (111 km by 111 km) aerogeophysical observations were made along orthogonal north–south and east–west profiles with a 5.3-km line spacing for each orientation. Given the average ice thickness of 2–3 km and a survey elevation of 0.5–1.5 km, this line spacing optimizes the recovery of topography from the ice-penetrating radar and unaliased gravity and magnetic measurements. The darkened

associated elevated heat flow beneath the WAIS near the critical region where ice streaming begins. If this heat flow is indeed controlling ice-stream formation, then penetration of ocean waters inland of the thin hot crust of the active portion of the West Antarctic rift system could lead to the disappearance of ice streams, and possibly trigger a collapse of the inland ice reservoir.

A West Antarctic rift system dominates the region of low-lying topography beneath the WAIS, the Ross Ice Shelf and the Ross Sea⁶ (Fig. 1). This region has experienced several periods of lithospheric extension beginning as much as 175 Myr ago, and possibly continuing through to the present⁷. The evidence for extension in the West Antarctic rift system is best developed in the Ross Sea, where the lithosphere is characterized by thin crust and sedimentary basins as well as recent volcanics^{8,9}. Both Marie Byrd Land and the Transantarctic Mountains are the sites of currently active volcanoes¹⁰. Active volcanism has not been identified within the Ellsworth–Whitmore crustal block, beneath the Ross Ice Shelf or beneath the WAIS. Because of the paucity of outcrop and the difficulty in conducting large-scale ground-based geophysics, few constraints exist on the nature and extent of the extensional processes that may dominate the low-lying topography beneath the WAIS.

As part of a programme entitled Corridor Aerogeophysics of the Southeastern Ross Transect Zone (CASERTZ), we have developed an aerogeophysical platform to study the interaction of geological and glaciological processes in West Antarctica. The aerogeophysical surveying during the 1991–92 field season (Fig. 1) revealed a distinct depression in the surface of the WAIS. This depression is underlain by a peak in the subglacial topography that is associated with a unique magnetic signature (Fig. 2). Located northwest of the Whitmore Mountains



circle within the survey area indicates the location of active subglacial volcanism. The dashed lines encompass the region thought to contain the inland edge of hot actively extending lithosphere inferred from the subglacial topography of Drewry¹⁷.

($81^{\circ} 52.6' S$ $111^{\circ} 18.1' W$), this feature is near the proposed southern flank of the rift system, and is ~ 100 – 200 km east and upslope of the initiation of ice streaming. The subglacial peak, which is 6 km wide at the base, rises 650 m above the surrounding topography to within 1,400 m of the ice surface (Fig. 2*b*, Fig. 3*a*). A blowup of the radar image (Fig. 3*b*) documents a steep-sided (12° slope) and slightly asymmetric morphology. Evaluation of nearby north-south and east-west profiles shows that this peak stands isolated as a central edifice in a 30-km region

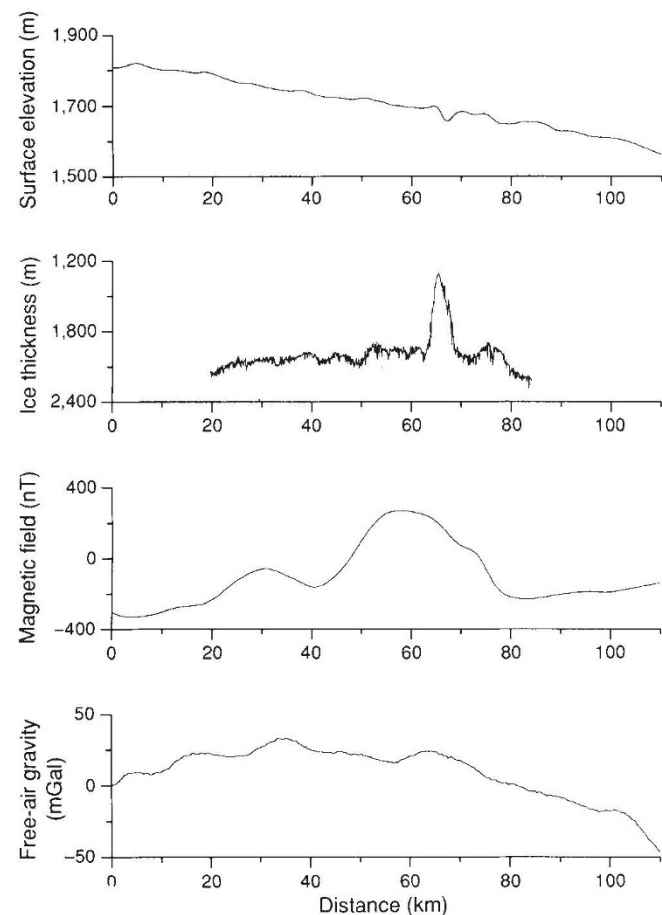


FIG. 2 Aerogeophysical observations made along one of our north-south profiles. The location of this profile is indicated in Fig. 4. These observations were collected from a de Havilland Twin Otter equipped with an ice-penetrating radar, a proton-precession magnetometer, an airborne gravity system and a laser altimeter. The aircraft is navigated by a local radio-transponder network while differential positioning techniques based on the Global Positioning System (GPS) satellites are used for recovering high-resolution horizontal and vertical positions. Attitude information from an inertial navigation system is used to correct the laser altimetry and a digital pressure transducer is used to recover vertical positions and accelerations in the absence of satellite positioning. *a*, Surface elevation from laser-altimeter measurements which have been corrected for aircraft attitude changes and combined with the altitude of the aircraft determined using differential satellite positioning techniques. The laser altimeter profiling of the ice surface is accurate to ~ 1 m. The anomalous depression in the ice surface is located at 67 km. *b*, Ice thickness automatically picked from the ice-penetrating radar observations of Fig. 3. The 60-MHz ice-penetrating radar can recover sub-ice topography with an accuracy of ~ 10 m through 2–3 km of comparatively warm West Antarctic ice. The peak of the central edifice is at 66 km and the rim of the proposed caldera intersects the profile at 53 and 76 km. *c*, Total magnetic field, accurate to several nanoTesla, corrected for ionospheric variations using observations from a fixed base station and with the geomagnetic reference field removed; the large anomaly between 40 and 80 km is strongly correlated with the volcanic construct which includes the caldera and central edifice of *b*. *d*, Free-air gravity profile, accurate to better than 5 mGal.

of elevated topography that is depressed in the center and bounded by a rim 100–200 m in height. The elevated region and its central edifice are characterized by a 600-nT positive magnetic anomaly, 40 km in diameter (Fig. 2*c*, Fig. 4*a*). The gravity signature is a 10-mGal anomaly centred over the edifice (Fig. 2*d*). The ice surface overlying the central edifice is characterized by a 48-m depression, ~ 6 km across and offset slightly to the south of the peak (Fig. 2*a*). The form of this surface depression is constrained both by the east-west profile, which intersects Fig. 2 at 68 km, and by satellite imagery. The orthogonal profile shows that this recess extends 12 km perpendicular to the profile of Fig. 2 and begins 2.5 km to the east, and upslope of the peak. The depression in the ice-sheet surface is visible as a closed feature on the advanced very-high-resolution radiometer (AVHRR) satellite image of the survey area (Fig. 4*b*).

We interpret the central edifice to be a recently active volcano associated with the hypothesized flank of the West Antarctic rift system along the Whitmore Mountains. The absence of the peak in the radar data from adjacent lines indicates that the proposed volcano is a cone-shaped feature and not a linear ridge. We further interpret the rim ringing the broadly elevated region as the signature of a 23-km-wide caldera. The large-amplitude, long-wavelength magnetic anomaly indicates that the entire elevated region is a volcanic construct.

The depression in the ice surface just south of the central edifice provides evidence for recent volcanic activity. In our survey area the ice flows down a western dipping slope (Fig. 1) largely perpendicular to the profile of Fig. 2. Thus the surface depression is not directly downstream of the central edifice and cannot be a simple response to its presence. The anticipated response of the ice flowing over an elevated topographic feature would be a bump on the ice surface upstream, possibly associated with a depression downstream¹¹. Contrary to this prediction, the depression that we observe is not only offset from the central edifice but extends eastward and upstream. For these reasons, the depression in the ice surface is not a response to sub-ice topography but instead indicates an increased flux of ice into a region of anomalous basal melting.

To estimate the basal heat flow, we conservatively assume that ice is entering the depression only from the north and south along about one-half of its length (6 km), and that the inward slope at the edges of the depression is ~ 0.005 . This slope assumption ignores the local increases caused by the bumps bounding the depression. A simple mass-flux calculation¹² based on the flow law for ice at -20°C shows that, to maintain this slope, $\sim 0.07\text{ km}^3$ of ice must be removed each year from the base of an ice sheet 2,000 m in thickness. The power required to melt this ice is 700 MW. If the central edifice represents an isolated hydrothermal vent 6 km in diameter, the heat flow at this vent is 25 W m^{-2} , whereas if the source area is the size of the surface depression itself ($\sim 6 \times 12$ km), the heat flow is 10 W m^{-2} . This range of 10 – 25 W m^{-2} exceeds typical continental heat flow by three orders of magnitude but is consistent with observations from other ice-covered volcanoes. In Iceland, the heat flux from a single caldera, estimated from the volume of water produced by eruptive events¹³, is 50 W m^{-2} . In Alaska, accumulation rates and the internal properties of the ice cap on top of the active caldera of Mount Wrangell¹⁴ were used to estimate a heat flux of 7 W m^{-2} .

Active subaerial and submarine volcanism has been documented within the West Antarctic rift system¹⁰. In Marie Byrd Land, large shield volcanoes 10–35 km in diameter and 1–2 km in elevation are often characterized by summit calderas of ~ 6 km in diameter. The narrow central edifice emplaced on the broad constructional feature we have identified is morphologically distinct from these subaerial Marie Byrd Land volcanics. The submarine volcanoes of the Ross Sea are similar in form to the central edifice although they are distinguished by shorter wavelength magnetic anomalies (less than 10 km). We believe the steep slope of the central edifice (12°) indicates that it was

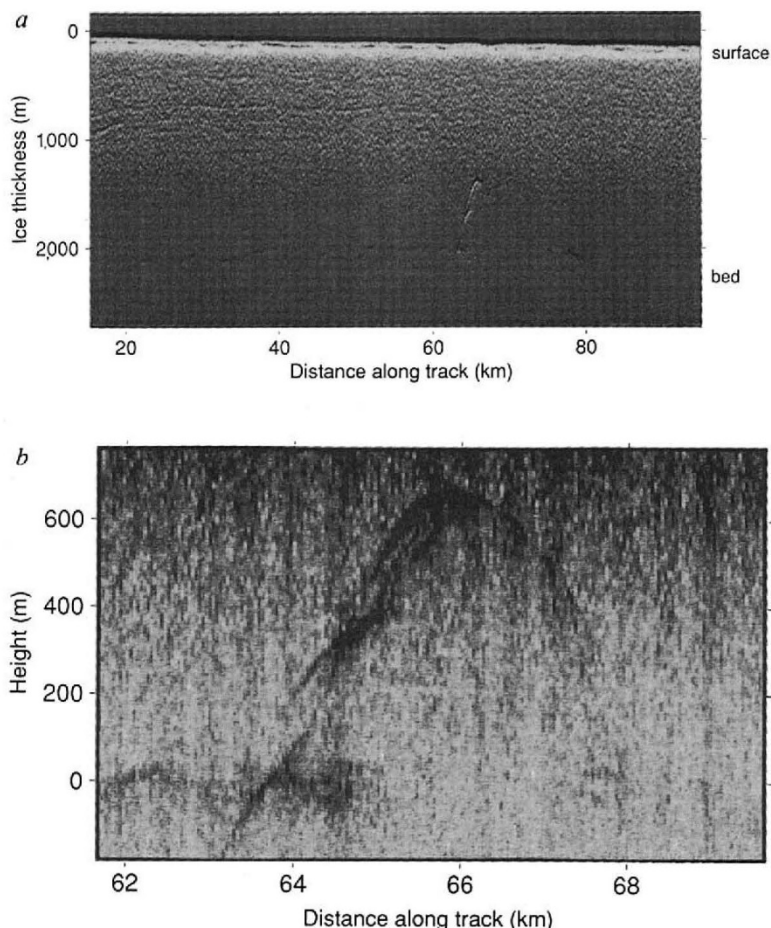


FIG. 3 Ice-penetrating radar observations made along the north-south profile designated by the arrows in Fig. 4. The horizontal scales are referenced to Fig. 2. a, The original observations used for Fig. 2b. Each of the 1,560 time-differentiated sweeps shown here represents the integrated result of 2,048 radar transmissions. The proposed volcanic construct between 50 and 80 km as well as the central edifice and its associated depression in the ice surface are clearly visible. In West Antarctica, radar echoes are often observed for thicknesses greater than 2,500 m so the weak signal strengths for thickness greater than 2,200 m probably result from an anomalously warm ice column. b, An expanded non-differentiated view of the central edifice. The north side of this steep-sloped feature is rugged as indicated by the tails of diffraction hyperbolae. The relatively smoother south side is characterized by weaker signal strengths which may indicate increased attenuation of radar transmissions resulting from elevated ice temperatures on this side of the proposed caldera.

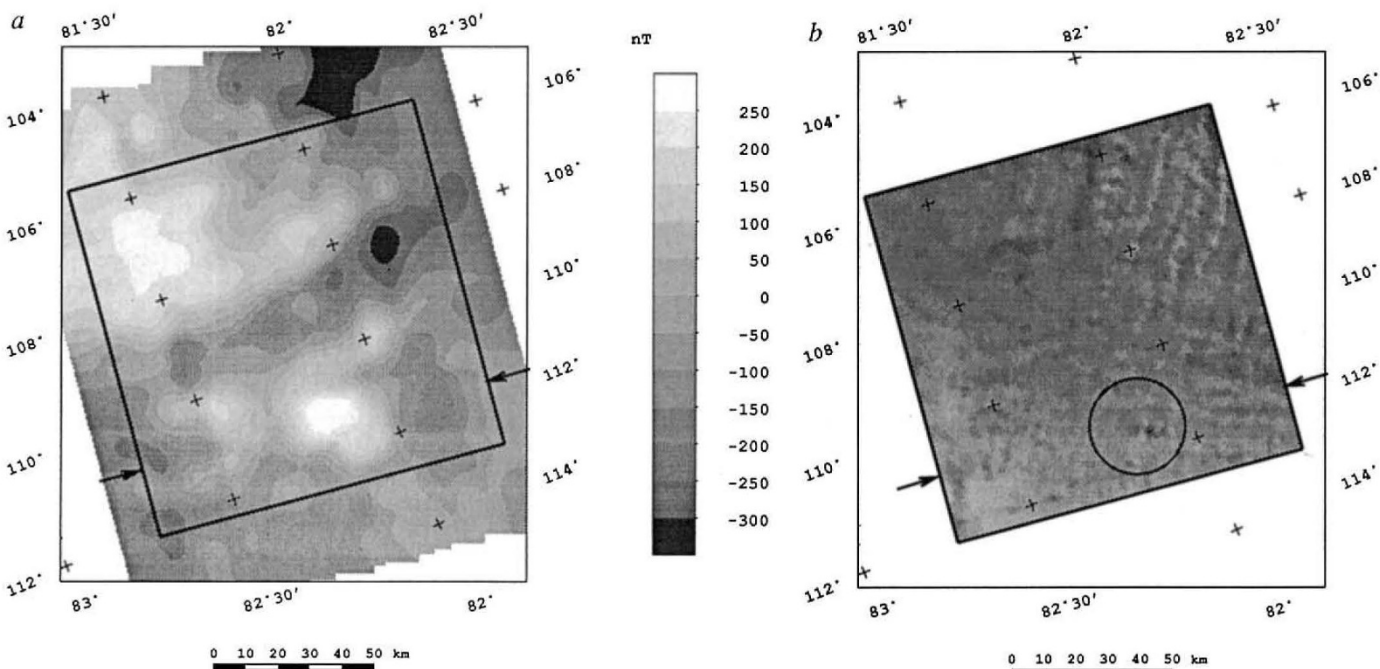


FIG. 4 a, Map of the total intensity of the magnetic field for the white survey block of Fig. 1 with a 50-nT contour interval. The arrows show the location of the profile used for Figs 2 and 3. A large kidney-shaped anomaly characterizes the volcanic construct that we have identified. The reduced amplitude for the lobe of the anomaly southwest of the central edifice likely indicates elevated crustal temperatures on this side of the proposed caldera.

b, AVHRR satellite imagery for 13 November 1991 at 0719 GMT over the same region as a. This image is illuminated from the south-southeast and AVHRR has a resolution of 1.1 km. A circle roughly the size of the proposed volcanic construct is positioned to include most of the kidney-shaped anomaly of a. The depression in the ice surface to the south of the central edifice is indicated by darker shading.

extruded into the ice or possibly underwater before the development of the WAIS.

Other satellite imagery over the ice streams and their catchment basins suggests that the volcano we have identified is not an isolated feature beneath the WAIS. Strikingly circular features in the Landsat images from ice stream E in West Antarctica¹⁵ might also be interpreted as volcanic constructs. The main implication of active volcanism beneath the ice is that elevated geothermal flux provides an important control on the dynamics of the WAIS. Spatial variations in geothermal flux will regulate the water supply available for saturating the sediment responsible for ice streaming. If the rifting process is providing the melt water and sediment required for ice streaming, then the ice streams may be unable to migrate beyond the edge of the active portion of the West Antarctic rift system. This edge would be a major geological boundary between thin hot actively extending lithosphere and cold inactive lithosphere. We believe such a boundary exists between the lithosphere of the interior Ross embayment, the relatively flat low-lying area between Marie Byrd Land and the Transantarctic Mountains, and the region dominated by the Ellsworth–Whitmore crustal block and the Byrd subglacial basin¹⁶. If the downstream terminus of the ice streams were to retreat to this geological boundary, then the reservoir of slow-moving inland ice would be exposed to the ocean without the buffer of the ice-stream system; this would almost certainly represent an unstable situation. Therefore, the character of the lithosphere within the central West Antarctic rift system and, specifically, the distribu-

tion of elevated heat flow and sedimentary basins, represents a fixed boundary condition for the WAIS that is independent of global climate yet could be responsible for triggering the collapse of the ice sheet. □

Received 22 October 1992; accepted 5 January 1993.

1. Mercer, J. H. *Nature* **271**, 321–325 (1978).
2. Thomas, R. H. *J. Glaciol.* **24**, 167–177 (1979).
3. MacAyeal, D. R. *Nature* **359**, 29–32 (1992).
4. Blankenship, D. D., Bentley, C. R., Rooney, S. T. & Alley, R. B. *Nature* **322**, 54–57 (1986).
5. Alley, R. B., Blankenship, D. D., Bentley, C. R. & Rooney, S. T. *Nature* **332**, 57–59 (1986).
6. LeMasurier, W. E. *Abstr. Progr.* **10**, 443 (Geological Society of America, 1978).
7. Wilson, T. J. *Antarct. J.* **25**, 31–34 (1991).
8. Davey, F. J. in *The Antarctic Continental Margin: Geology and Geophysics of the Western Ross Sea*, 1–16 (Circum-Pacific Council for Energy and Resources, Houston, 1987).
9. Behrendt, J. C., Cooper, A. K. & Yuan, A. in *The Antarctic Continental Margin: Geology and Geophysics of the Western Ross Sea*, 155–177 (Circum-Pacific Council for Energy and Resources, Houston, 1987).
10. LeMasurier, W. E. & Thomson, J. W. (eds) *Volcanoes of the Antarctic Plate and Southern Oceans* (American Geophysical Union, 1990).
11. Robin, G. de Q. *Nature* **215**, 1029–1032 (1967).
12. Paterson, W. S. B. *The Physics of Glaciers* (Pergamon, Oxford, 1981).
13. Björnsson, H. *Jökull* **33**, 13–18 (1983).
14. Clarke, G. K. C., Cross, G. M. & Benson, C. S. *J. geophys. Res.* **94**, 7237–7249 (1989).
15. Bindshadler, R. A. & Scambos, T. A. *Science* **252**, 242–246 (1991).
16. Dalziel, I. W. D. & Elliot, D. H. *Tectonics* **1**, 3–19 (1982).
17. Drewry, D. J. *Antarctica: Glaciological and Geophysical Folio* (Scott Polar Research Institute, Cambridge, 1983).

ACKNOWLEDGEMENTS. We thank K. Najmulski, K. Griffiths, M. Noonan, V. Childers, J. Jarvis, S. Doppelhammer, R. Arko, M. Peters, K. Killilea, J. Peryea, R. Campbell and the personnel of Ken Borek Air Ltd. for their long-term technical support. The work was improved by helpful comments from I. W. D. Dalziel, R. B. Alley, and D. R. MacAyeal. This work was supported by the Division of Polar Programs of the U.S. NSF.

Seismological mapping of fine structure near the base of the Earth's mantle

John E. Vidale & Harley M. Benz

United States Geological Survey, 345 Middlefield Road, Menlo Park, California 94025, USA

THE Earth's core–mantle boundary (CMB) juxtaposes liquid iron and crystalline silicates, and is a region of large vertical thermal gradients. The D'' region, which extends up to 200–300 km above the CMB, often has elevated shear-wave velocity and suggestions of lateral variations in structure¹. Recent improvements in our ability to assemble and analyse records from regional seismic networks have allowed us to examine long profiles of travel times, amplitudes and waveforms from more than a thousand short-period seismometers². We observe, across Canada and the United States, P waves that have grazed the CMB from the powerful nuclear test in Lop Nor, China, on 21 May 1992. First-arrival travel times and large secondary arrivals are consistent with a 1.5% compressional velocity increase with depth ~ 130 km above the CMB—about half the thickness of D'' in this locality³. Our observations, together with evidence for the absence of such a thin, fast layer in neighbouring regions, suggest the presence of lateral heterogeneity in composition or phase at the base of the mantle.

Discrimination between the various thermal and compositional explanations of heterogeneity at the base of the mantle requires knowledge of variations in the velocity of both compressional (P) and shear (S) waves. The D'' layer is laterally heterogeneous^{1,4–8}: some studies find a sudden increase with depth in the P- and S-wave velocities 200–300 km above the CMB^{1,6–11}, whereas others infer smoother velocity variations^{6,12}. A P-wave velocity decrease in the deepest 100 km of the mantle has also been inferred^{10,13,14}, suggesting a thermal boundary layer^{15,16}.

The nuclear explosion at Lop Nor, China, with a yield of 0.66 Mt (megatonnes high explosive equivalent) (21 May 1992, 41.55° N 88.84° E, 1.6 km deep, $m_b = 6.5$; L. Gao and T. C. Wallace, personal communication), provided a large, impulsive P-wave source. It has been more than 10 years since the last explosions of this size, and the seismic networks at that date were much more sparse. The size of the Lop Nor explosion allows us to see short-period P waves diffracting into the distances of the core shadow, and its brief duration allows us easily to isolate multiple arrivals separated by only 1–2 s. By assembling many records from a single event, we avoid the problem faced by previous researchers of how to combine records of an array of events, with generally unknown origin-time errors, mislocations and amplitude calibration between events.

We use the digital short-period seismograms from 14 regional networks in the United States and Canada¹⁷ to investigate the structure above the CMB. The P waves graze the core between the sections of the CMB beneath northern Alaska and Greenland (Fig. 1). The 477 seismograms with the lowest background and signal-generated noise levels were chosen from a total of 1,062 available.

Figure 2 shows seismic sections of stations in three narrow azimuthal ranges. The P wave is simple in the range from 80° to 92°. Later arrivals appear in the distance range from 92° to 103°, which vary in timing and amplitude with azimuth from the explosion. A clear arrival with slightly smaller amplitude follows the P wave by 1–3 s in each profile. Much less distinct later arrivals are seen for profiles across the eastern third of North America. This secondary arrival is not due to scattering near the receivers, as it is absent in earthquakes that we have examined and it is similar for nearby stations. It does not arise from source complexity, as it is absent in the distance range from 80° to 92°.

The secondary arrival is travelling 0.25 s deg^{-1} more slowly than the initial P arrival. Figure 3a presents the first and secondary arrival times. The pattern is typical of an abrupt increase in velocity with depth: the slowness (reciprocal apparent velocity) of the first arrival decreases abruptly from 5.0 s deg^{-1} in the